Phytochemistry 71 (2010) 531–542

Contents lists available at ScienceDirect

Phytochemistry

journal homepage: www.elsevier.com/locate/phytochem

Consequences of antisense down-regulation of a lignification-specific peroxidase on leaf and vascular tissue in tobacco lines demonstrating enhanced enzymic saccharification

Bahram Kavousi [a], Arsalan Daudi [b], Charis M. Cook [b], Jean-Paul Joseleau [c], Katia Ruel [c], Alessandra Devoto [b], G. Paul Bolwell [b], Kristopher A. Blee [a,*]

[a] Department of Biological Sciences, California State University, Chico, CA 95929, USA
[b] School of Biological Sciences, Royal Holloway, University of London, Egham, Surrey TW20 0EX, UK
[c] Centre de recherche sur les macromolecules vegetales, UPR CNRS 5301, BP53, 38041 Grenoble, France

ARTICLE INFO

Article history:
Received 18 September 2009
Received in revised form 17 December 2009
Available online 17 February 2010

Keywords:
Tobacco
Nicotiana tabacum
Peroxidase
Antisense
Cell wall
Saccharification
Photosynthesis

ABSTRACT

Tobacco plants expressing an antisense construct for a cationic peroxidase, which down-regulated lignin content at the presumed level of polymerisation, have been further analysed. T_1 plants were derived from a large-scale screen of T_0 mutant lines, previously published, which identified lines demonstrating consistent lignin down-regulation. Of these, line 1074 which had the most robust changes in lignin distribution through several generations was shown to have accompanying down-regulation of transcription of most lignin biosynthesis genes, except cinnamoyl-CoA reductase. The consistent 20% reduction in lignin was not accompanied by significant gross changes in vascular polysaccharide content and composition, despite a modest up-regulation of transcripts of genes involved in cellulose and hemicellulose synthesis. Morphologically, 1074 plants have under-developed xylem with both fibers and vessels having thin cell walls and limited secondary wall thickening with an abnormal S2 layer. However, they were not compromised in overall growth. Nevertheless, these and other lines showed improved potential industrial utility through a threefold increase in enzymic saccharification efficiency compared with wild-type (wt). Therefore, they were profiled for further un-intended effects of transgenesis that might compromise their value for industrial or biofuel processes. Other phenotypic changes included increased leaf thickness and bifurcation at the tip of the leaf. wt-Plants had smaller chloroplasts and higher stomatal numbers than mutants. Transgenic lines also showed a variable leaf pigment distribution with light-green areas that contained measurably less chlorophyll a, b, and carotenoids. Changes in epidermal pavement cells of mutant lines were also observed after exposure to various chemicals, while wt leaves retained their structural integrity. Despite these changes, the mutant plants grew and were viable indicating that lignification patterns can be manipulated considerably through targeting polymerisation without serious deleterious effects.

Published by Elsevier Ltd.

1. Introduction

The efficiency of extraction and recovery of cellulose from plant cell walls influences many industrial processes including fiber production, pulp and paper-making and utilisation of biomass for biofuel. The biomass with the highest industrial applicability is mainly derived from secondary walls, which consist of three distinct layers (S1, S2, S3), easily distinguishable at an ultrastructural level from differences in the orientation of their cellulose microfibrils. The transition from primary to secondary cell wall synthesis is marked by the cessation of pectin deposition and a noted increase in the synthesis and deposition of cellulose/hemicellulose and lignin. Lignin and xylans limit the efficiency of cellulose extractability and have therefore been targets for genetic manipulation to improve such processes with consequent environmental benefits. Also these studies, whose primary purpose was manipulation of lignin content and composition in plants, has also led to increased understanding of the extent of co-assembly of the three distinct major polymers in secondary walls (reviewed in Boudet et al. (2003),

Abbreviations: ADH, bifunctional alcohol/UDP-glucose dehydrogenase; AIM, acetone-insoluble material; CES3A, cellulose synthase; CSLD, cellulose synthase-like D; PAL, phenylalanine ammonia lyase; C4H, cinnamate 4-hydroxylase; C3H, coumaroyl-ester-3-hydroxylase; COMT, caffeic acid *O*-methyl-transferase; CCOMT, caffeoyl-CoA *O*-methyl-transferase; CCR, cinnamoyl-CoA reductase; CAD, cinnamyl alcohol dehydrogenase; SUSY, sucrose synthase; UGD, UDP-glucose dehydrogenase; UXS, UDP-glucuronate decarboxylase.

* Corresponding author. Tel.: +1 530 898 5116.
E-mail address: kblee@csuchico.edu (K.A. Blee)

0031-9422/$ - see front matter Published by Elsevier Ltd.
doi:10.1016/j.phytochem.2010.01.008

Anterola and Lewis (2002), Boerjan et al. (2003), and Vanholme et al. (2008)). Although the majority of the engineering was aimed at structural genes in phenylpropanoid and monolignol biosynthesis and the transcription factors controlling their expression, the polymerisation process has also been targeted by antisense manipulation of vascular-specific peroxidase with significant down-regulation of lignin levels (Blee et al., 2003). All this resource now requires detailed analysis for un-intended effects of transgenesis. This is particularly relevant to peroxidases due to their diverse roles in the plant.

The plant peroxidase superfamily is divided into three classes (I, II, III) based on their primary structure sequence similarities (Welinder, 1992). The class III peroxidases are abundant in plant tissues, they are secreted enzymes found in extracellular space or in vacuoles with multiple functions such as biosynthesis of cell walls, lignification, auxin catabolism, suberization, defense responses, as well as response to environmental stresses, and hydrogen peroxide detoxification (Tognolli et al., 2002; Duroux and Welinder, 2003; Valerio et al., 2004; Passardi et al., 2004, 2005; Marjamaa et al., 2009). Class III peroxidases are readily detected in the proteome of secondary walls of tobacco xylem where they are implicated in lignin polymerisation, but as they co-localise with a number of PR (pathogenesis-related) proteins, it has also been suggested they are involved in defence by anticipating potential ingress of pathogens through the vascular system (Millar et al., 2009). In addition to xylem, lignin is present in the cell walls of sclerenchyma, phloem, and peridermal tissues (Lewis and Yamamoto, 1990). The related polymer, suberin, is also a cell wall component consisting of both polyphenolic and polyaliphatic domains. Suberin is synthesized in the endodermis and exodermis of the root where it strengthens the cell wall and helps in water retention and movement (Bernards et al., 1999; Bernards, 2002). The last catalytic step in the synthesis of lignin and the aromatic domain of suberin is the one electron oxidation of cinnamyl alcohols and hydroxycinnamates, which is believed to be performed by peroxidase (Anterola and Lewis, 2002; Bernards et al., 2003). Thus manipulating peroxidases might also have consequences for water relations in all these tissues.

Previous studies have also implicated peroxidases in diverse metabolic and developmental processes, which also indicates their potential for less direct un-intended effects. Many developmental changes are highly regulated in part by auxin, including cell expansion, cell division, vascular tissue differentiation, root development, phototropism, fruit ripening, flowering and leaf senescence (Bartel, 1997). Analysis of IAA degradation products indicates that peroxidases play an important role in auxin catabolism through oxidative decarboxylation (Gazaryan et al., 1998). In transgenic tobacco over expressing anionic peroxidase, IAA levels were lower, stomata closed and root branching reduced (Gazaryan and Lagrimini, 1996; Lagrimini et al., 1997a). Elevated IAA levels in plants with suppressed anionic peroxidase via antisense RNA, resulted in rapid shoot growth and shorter flowering time and fused leaves (Gazaryan and Lagrimini, 1996; Lagrimini et al., 1997b).

Chloroplasts are generators of oxygen due to photosystems and eventual producers of reactive oxygen species (ROS), where the D1 protein of PSII is a major target for damage (Keren et al., 1997). PSI is also susceptible to damage from active oxygen species due to the strong reducing capacity of the ferredoxin acceptor of PSI, which readily reduces molecular oxygen to form superoxide. Reduction of oxygen competes with the reduction of $NADP^+$ and the normal channeling of electrons (Asada, 1999). Chlorophyll itself will be a target for such ROS and therefore intact chloroplasts contain large amounts of peroxidase activity which is catalysed primarily by the class I ascorbate peroxidase. This is in order to detoxify hydrogen peroxide (Mehlhorn et al., 1996), but class III peroxidase may also contribute to regulating H_2O_2 as it is considered to be readily diffusible.

Previously, considerable work was carried out on the possible role of tobacco anionic peroxidase in lignification (Lagrimini, 1991; Lagrimini et al., 1997a,b). We explored the function of cationic peroxidases through use of a cDNA coding for FBP1, a cationic cell wall peroxidase from French bean, to isolate TP60, a cDNA encoding a cationic cell wall peroxidase expressed during secondary growth in stems from tobacco. Transgenic tobacco plants were produced and antisense constructs for both peroxidases silenced a specific cationic peroxidase activity in stems resulting in down-regulation of lignin (Blee et al., 2003). During maintenance and generation of T_1 and "homozygous" plants for allotetraploid tobacco, a number of phenotypic abnormalities in the leaves have been found to persist. These included bifurcation of the leaf tip in line 1074, the presence of light green patches on leaf surfaces in line 113, as well as increased thickness of the leaves of the transformants indicating differential effects in other tissues.

The present work analyses the consequences of cationic peroxidase down-regulation in greater detail. We report direct cell wall changes and consequences for lignin and polysaccharide content resulting in improved enzymic saccharification. However, there could also be additional consequences to lignin down-regulation since reduced photosynthetic capacity and photo-oxidative stress have already been noted in antisense CCR, CAD and double transformants of tobacco (Dauwe et al., 2007). The observed changes in leaf pigmentation in the peroxidase down-regulated plants could imply mesophyll/chloroplast/chlorophyll modifications, possibly as a result of reactive oxygen species accumulation due to reduced peroxidase activity. Therefore, we investigated potential changes to the photosynthetic capacity of these plants. Because peroxidase activities support both loosening of cell walls and growth by expansion, as well as cross-linking of cell wall components and an imposed limit to cell expansion (Passardi et al., 2004, 2006), we also monitored cell shape and report anatomical changes in the transformants that support potential roles for the silenced peroxidases in cell growth and shape.

2. Results

2.1. Morphological characteristics of transformed tobacco lines

T_1 tobacco plants carrying the peroxidase antisense silencing construct displayed several phenotypical differences in comparison to wild type (wt) plants (Fig. 1). At equivalent stages of development, transformed lines 76 and 113 were consistently shorter in height than wt-plants. Leaves from lines 76, 113, and 1074 displayed obvious abnormalities in coloration in the form of light green patches that appeared apparently randomly on either the adaxial leaf surface or leaf margin. Transformed lines produced leaves with indentations along the margins at positions where vascular tissue meet the leaf edge, especially near the leaf apex. Leaves from transformed plants sometimes produced a forked mid-vein and two apices. Morphological abnormalities displayed by the transformants included an unusual thickening of the leaf blade at all stages of development examined, especially in mutants 113 and 1074, followed by 76 (Fig. 2). An ANOVA of mean leaf thickness indicated an effect of the presence of the antisense peroxidase construct ($p = 0.011$, Table 1). Statistical pair wise comparison of mean leaf thickness identified significant differences between the leaves of line 113 and wt leaves at node 10, 1.29 mm versus 0.405 mm, respectively ($p = 0.014$, Table 1).

2.2. Anatomical analysis of vascular tissue within stems

Morphological aspects of stems from wt and transformants (lines 1074 and 1120) displayed phenotypic differences (Table 2),

Fig. 1. Appearance of wild type and peroxidase-antisense-silencing-construct-carrying tobacco plants. Top panel from left to right: wt and transgenic plants 76, 113, and 1074. Middle panels represent mutant 113 with light green patch phenotype visible on the upper leaf surface near the leaf margin (middle right) and within the leaf blade (middle left). Lower panels represent mutant 1074 with bifurcation of the tip.

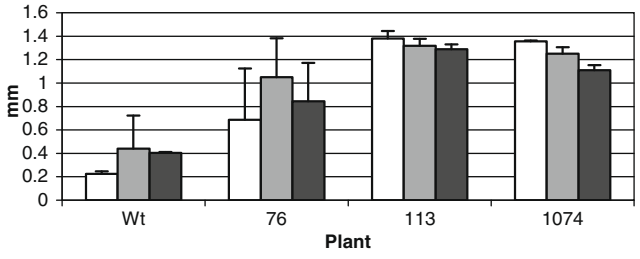

Fig. 2. Average thickness of developing leaves from wild type and transgenic plants. White bars represent leaf thickness at node 4, gray bars represent leaf at node 7 and black bars represent leaf at node 10. Values displayed for leaves at nodes 4, 7 and 10 represent averages from two to three measurements, each from a separate plant. Error bars represent +1SD.

Table 1
Statistical analysis of leaf thickness at node 10 data as shown in Fig. 2.

	Sum of squares	df	Mean-square	*F*-ratio	*p*
One-way ANOVA					
Between groups	1.026	3	0.342	9.244	0.011
Plant	1074	113	76		wt
Bonferroni matrix of pairwise comparison probabilities of leaf thickness at node 10					
1074	1.000				
113	1.000	1.000			
76	1.000	0.176	1.000		
wt	0.063	0.014	0.280		1.000

with the stems of line 1074 being more slender than the wt and line 1120. Interestingly in the line 1074, which has a 23% reduction in lignin (Blee et al., 2003), a reduction of xylem development of about 28% on a dry weight basis was observed (Table 2). In line 1074, this was accompanied by a reduction in number of vessels (Fig. 3), and a striking enlargement in diameter of surrounding fibers, while xylem of line 1120 appeared unaffected. Secondary wall thickness appeared reduced in vessels of mutant lines (Fig. 3). This observation was confirmed with TEM where, although no conspicuous modification of line 1074 fibers could be found, vessels did possess a thin cell wall with a very limited secondary wall thickening with an abnormal S2 layer in comparison to the wt (Fig. 4).

2.3. Immunological localisation of lignin epitopes

Ten lines were previously subjected to complete chemical analysis of lignin of which 1074 had a 23% overall reduction (Blee et al., 2003), while 1120, analysed subsequently, did not show any significant reduction in lignin content as compared to controls (unpublished data). These have now been examined by immunocytology of lignin epitopes (Fig. 4). The consequences of the antisense transformation appear to be tissue specific within the whole xylem with vessels and fibers differently affected and no modification of ray cell walls. Both vessels and fibers displayed elevated proportions of syringyl epitopes as compared to wt, particularly in the S2 of fibers from line 1074 (Fig. 4B). The detection of syringyl residues in vessels is novel since this lignin is usually considered to be guaiacyl-rich; however, syringyl residues have been occasionally reported in some types of vessels (Donaldson, 2001). By comparison, down-regulated CCR tobacco lines showed major changes in S2 with the characteristic loosening of fiber associations (Chabannes et al., 2001a,b; Ruel et al., 2001), and there was a conspicuous lack of syringyl residues in this layer in the corresponding poplar transgenics (Leplé et al., 2007). Homoguaiacyl 'condensed' epiotopes, on the other hand, were strongly reduced in the S3 of fibers from 1074, only weakly so in the S1. However, within vessel walls of line 1074, the inner part of S2 and S3 became richer in the 'condensed' guaiacyl subunits (Fig. 4D).

2.4. Polysaccharide analysis

The procedure for determining polysaccharide composition of tobacco secondary walls [72% (v/v) H_2SO_4 (6 h, 20 °C) rather than 72% (v/v) H_2SO_4 (30 min, 30 °C)] was optimized for maximum hydrolysis of cellulose without excess sugar degradation. Neutral sugar analysis of acetone-insoluble material (AIM) from xylem cell walls in wt and down-regulated lines 1074 and 1120 showed a

Table 2
Vascular morphology of stems from wild type and transgenic lines. The first internode from stems from plants were sampled at three locations, the upper most region (U), the middle (M), and the lower region (L) reflecting progressive maturation of the cell wall. Xylem is expressed as percent of the whole dry stem material.

Tobacco line	Stem location	Xylem (%)	Phenotype
wt	U	48	Thin
	M	61.5	Thin; soft
	L	70	Thick; resistant to cutting
1074	U	50.5	Resistant to cutting
	M	50.5	Thin; soft
	L	ND	Very thin (??)
1120	U	55.5	=wt
	M	67	=wt
	L	71.5	Resistant to cutting

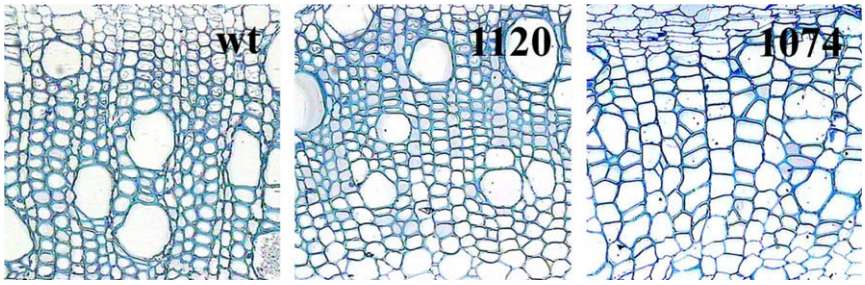

Fig. 3. Vessel morphology and density in stem tissues. Toluidine blue staining of transverse sections through equivalent stems of wild type and transformed lines revealing files of cells generated by the vascular cambium during secondary growth. The vascular cambium is oriented to the upper side or upper side and just off field of view for all panels. All panels are of equal magnification.

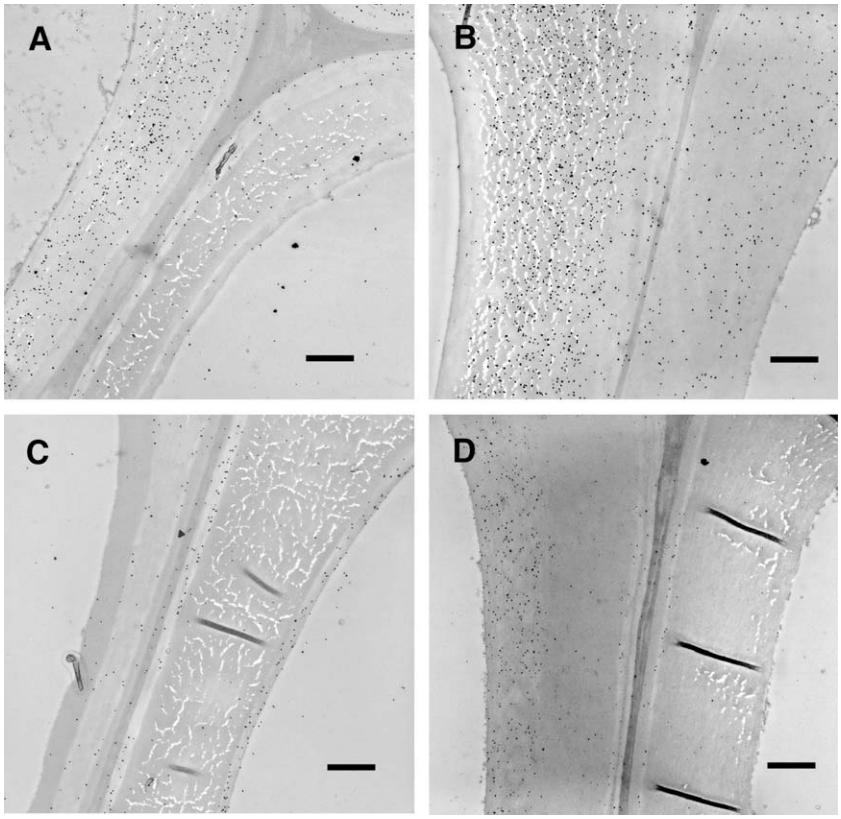

Fig. 4. Fiber and vessel ultrastructure and immunocytochemical characterisation of lignin. Tissue sections of upper panels probed for syringyl epitopes and tissue sections of lower panels probed for homoguaiacyl condensed epitopes. (A) and (C), wt; (B) and (D), 1074. Cell wall layers S_1, S_2, and S_3; fibers F; and vessels V. Bars = 1 μm.

range of 45–50% glucose and 21–24% xylose (Table3). This compares with the same analysis on poplar, which gave 48% glucose and 25% xylose (Leplé et al., 2007). No significant modifications in the polysaccharide composition were detected between the lines. In contrast, walls analysed in separate batches and at the same time from xylan-down-regulated lines showed significant increase of glucose/xylose ratios (Bindschedler et al., 2007). Other neutral sugars contributed less than 4% in total indicating little glucomannan and other generic polysaccharide content in tobacco xylem and are omitted to simplify the data. Glucose and xylose are indicative of the corresponding cellulose and xylan hemicellulose in the cell walls between the upper, the middle part, and the lower part of the stem internode, and represent composition of the cell wall as it matures. In two sets of samples corresponding to two different pools of line 1074 and of line 1120, no significant variation in the carbohydrate analysis could be observed. Thus there was no compensatory increase as reported for cellulose as a consequence of monolignol engineering in tree species (Hu et al., 1999; Leplé et al., 2007). There may be different feedback mechanisms in plants affected in the provision of monolignols rather than in the polymerisation process as in these lines.

2.5. Enzymic saccharification efficiencies of selected lines

AIM from dissected xylem tissue from line 1074 was subjected to enzymatic digestion without chemical pre-treatment. Fig. 5 shows the release of reducing sugars over a 72 h period expressed as mol released/total carbohydrate in AIM to account for the consequence of the 20% reduction of lignin in the total dry weight. The amount of sugars released account for 55% of total carbohydrate from the 1074 lines as compared with 22% from wt lines. This compares favourably with data from alfalfa (Chen and Dixon, 2007) and demonstrates the utility of reducing lignin through targeting

Table 3
Cellulose/hemicellulose ratio of wild type and transgenic lines. The lowest internode of stems were sampled at three locations, the upper most region (U), the middle (M), and the lower region (L) reflecting progressive maturation of the cell wall. The values are the mean of three assays.

Tobacco line	Stem location	Yield of neutral sugars from total AIM (%)	Xylose (%)	Glucose (%)	Glc/ Xyl
wt	U	70.4	23.8	45.1	1.9
	M	69.5	20.7	47.6	2.3
	L	73.6	23.9	47.7	2.0
1074	U	69.3	21.4	44.5	2.1
	M	72.8	22.4	48.1	2.15
	L	73.6	22.7	50.6	2.2
1120	U	68.2	22.3	42.9	2.1
	M	70.8	22.3	46.5	2.15
	L	72.8	21.2	49.2	2.2

of lignin peroxidase. Improved saccharification was also found for homologous line 1135 and heterologous line 113.

2.6. Gene expression

A collection of ESTs (accession numbers EH663598–EH666265) has been made from a xylogenic tobacco cell culture (Blee et al., 2001b). As a result of annotation and array analysis (data not shown), genes were identified which were specifically expressed in the lignin, cellulose and xylan pathways in these xylogenic cells (Table 4). Internodes (1–6) showing maximum expression of secondary wall-related genes (Bindschedler et al., 2005) were profiled under an agreed protocol (see Section 5). qRT-PCR was performed on pooled RNA samples from stems of wt and 1074 and fold difference in expression calculated (Fig. 6). All the genes of lignin biosynthesis that could be identified in the EST were down-regulated, with the exception of COMT and CCR which were up-regulated. However, CoA esters of monolignols can be precursors of conjugates other than lignin in tobacco. All the genes found to be down-regulated were also down-regulated in AsCCR and AsCAD tobacco plants and the double transformants (Dauwe et al., 2007) so this seems to be a feature of lignin down-regulated lines in tobacco. In contrast, the CesA3 cellulose synthase homologue, which appears to be xylem-specific in tobacco, and genes involved in xylan synthesis in tobacco (Bindschedler et al., 2005) were all up-regulated. However, this was not to the extent that there was any

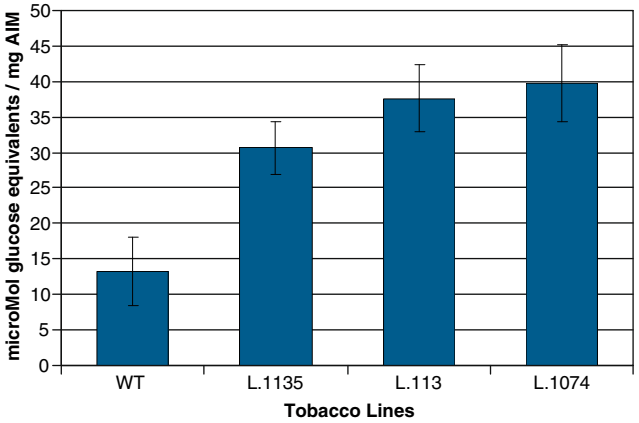

Fig. 5. Saccharification efficiency of lines 113, 1074, and 1135. AIM of pools of stems consisting of the bottom six internodes was subjected to saccharification for 72 h. The data for three determinations from six separate pools of internodes from different plants are shown, i.e., 18 determinations with SD.

eventual compensatory increased accumulation of these polysaccharides detected in the mature xylem of internode 1 (Table 3).

2.7. Consequences on leaf anatomy and physiology

After sample preparation for EM viewing, adaxial epidermal pavement cells from the different transformed lines consistently demonstrated a differential phenotypical response to the chemicals used in the SEM protocol as compared to wt. The leaves were all prepared similarly (see Section 5) then critical point dried in identical time intervals. Epidermal pavement cells of wt-plants appeared normal. In leaves from nodes 7, pavement cells of lines 76 and 113 displayed shrinking. Pavement cells of line 1074 appeared similar to wt (Fig. 7).

Examination of wt leaf mesophyll revealed typical columnar palisade parenchyma followed abaxially by vascular bundles with spongy parenchyma (Fig. 8). In mutants 113 and 1074, the epidermis is visible along with vascular bundles surrounded by mesophyll, but development of palisade parenchyma is absent (Fig. 8, left panel). Examinations of additional leaves from the same 113 and 1074 plants revealed palisade parenchyma cells were also present (Fig. 8, right panel).

Though not significantly so, chlorophyll and carotenoid content in leaves of the transformed lines 76, 113, and 1074 were equal to or elevated in comparison to wt levels in leaves from nodes 3 and 9 (Kavousi and Blee, unpublished results). Considerably elevated levels of chlorophyll a and b and carotenoids were noted in AsCCR and AsCAD and double transformant lines of tobacco (Dauwe et al., 2007). However, in antisense peroxidase lines such as 113, reduced chlorophyll a, b, and carotenoid contents were found within the light green patches as compared to pigment abundance in adjacent dark green areas from the same leaf (Table 5). The reduction of pigments within the light-green areas was most pronounced in the leaves from nodes 4 and 7 with light-green areas from the node 4 leaf yielding chlorophyll a, b, and carotenoids at 35.95, 19.70, and 9.27 $\mu g\ cm^{-2}$ compared to dark green areas at 56.54, 27.13, and 15.63 $\mu g\ cm^{-2}$, respectively. Pigment ratios for light green patches versus dark green areas for chlorophyll a to b (chl a/b) were 1.82 versus 2.08, respectively, and for the combined chlorophylls to carotenoids (chl/c) 6 versus 5.35, respectively.

Carbon assimilation rates in the mutants were slightly lower than wt rates in the majority of leaves examined (Fig. 9). An ANOVA indicated a significant effect on leaves at node 5 ($p = 0.007$, Table 6). In comparison to the wt assimilation rate of 12.8 $\mu mol\ CO_2\ min^{-1}\ cm^{-2}$ for leaves at node 5, mutant leaves of the same position produced significantly lower rates of 11.2 $\mu mol\ CO_2\ min^{-1}\ cm^{-2}$ for line 76 ($p = 0.032$) and 10.1 $\mu mol\ CO_2\ min^{-1}\ cm^{-2}$ for line 1074 ($p = 0.012$). Although the analysis chamber of the Li-Cor 6400 was too large to allow determination of assimilation rates for leaf areas within light green patches occurring on mutant leaves, measurements using the 1 cm chamber were conducted that included the light green patches and adjacent dark green areas. The results indicate slight differences in photosynthetic capabilities between leaf area that included a light green patch and area within the same leaf that did not contain light green patches. Marginally lower rates of carbon fixation were detected in light green containing areas of leaves from mutant 113, 10.6 $\mu mol\ CO_2\ min^{-1}\ cm^{-2}$ as compared to11.56 $\mu mol\ CO_2\ min^{-1}\ cm^{-2}$ for adjacent dark green areas at node 7 (Table 5).

When stomatal conductance was examined, no effect of treatment was detected (data not shown). However, stomatal densities on the abaxial leaf surface were greatly reduced in all the mutant lines. The highest stomatal densities observed were from wt leaf surfaces with 165 stomata mm^{-2} followed by mutant 76 with 156 stomata mm^{-2}, mutant 113 with 91 stomata mm^{-2}, and mutant 1074 with 69 stomata mm^2 (Fig. 10). ANOVA indicated an

Table 4
Quantitative real-time RT-PCR primers used in this study.

Gene	EST/clone	Forward (5′ to 3′)	Reverse (5′ to 3′)	Size (bp)
ces3a	EH663724	TGGAATTGATGAATGGTGGA	CAACCCTTGGAAGACCTAGC	90
pal	D17467	GCAAACAGCTCAATCTTCCA	TCGACTTCTTTTGGCAACAC	74
c4h	EH664914	AGCAATGCTCTGAAATGTGC	CCTCAGTTGATCTCCCCTTC	67
comt	EH663855	ACATAACCCAGGAGGCAAAG	TTCCATGACCCAAGTGTTGT	114
ccomt	EH665253	ATTTTCGTGGATGCTGACAA	GTCGTAGCCAATCACACCAC	90
c3h	EH663728	AGCAGTGGCCTTTAACAACA	GTCACCATCACACTTCAAAGG	75
ccr	AY149609	TGTGTCTTCTGTTGCTGCTG	ATTCACTGTCCGACCAACAA	83
cad	EH664196	TGGAACATCTTGGTGCAGAT	ATGGCCAACAGGGACAGTAT	107
susy	EH664745	GAAGCAAGGACACTGTTGGA	ATACAATCCAGGCATCGTGA	62
ugd	EH663670	AATGAGTCCAACAACCGTGA	TCCTTTGTTGCTGTGTAGGC	63
adh	AY619949	AATGCCATGTCAGCTCTTTG	AGCATATGCCACCTGTGAGA	60
uxs1	EH663981	AAAACCACCACCAGAACCAT	CAATAAATCCAGCACCACCA	93
uxs4	AY619953	TTGCCCGAATTTTCAATACA	CTGGGAAACAAAGTTGCTGA	77
csld	EH665280	GGAAAGGAACTTGGAAGTGG	AATCTGCACAATCCCACGTA	80
prx	AF149251	CTTGCCAACAAGCTCCACTA	CAAAGGAAGGGGAAAAGTGA	76

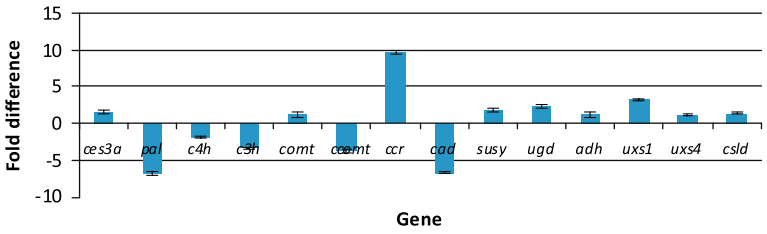

Fig. 6. Transcriptional consequences of lignin down-regulation in line 1074. qRT-PCR was performed for xylem-specific transcripts involved in (a) cellulose [cellulose synthase *ces3a*], (b) lignin [phenylalanine ammonia lyase (*pal*), cinnamate 4-hydroxylase (*c4h*), coumaroyl-ester-3-hydroxylase (*c3h*), caffeic acid *O*-methyl-transferase (*comt*), caffeoyl-CoA *O*-methyltransferase (*ccomt*), cinnamoyl-CoA reductase (*ccr*), cinnamyl alcohol dehydrogenase (*cad*)], and (c) xylan [sucrose synthase (*susy*), UDP-glucose dehydrogenase (*ugd*), bifunctional alcohol/UDP-glucose dehydrogenase (*adh*), UDP-glucuronate decarboxylase (*uxs*), cellulose synthase-like D (*csld*)] biosynthesis.

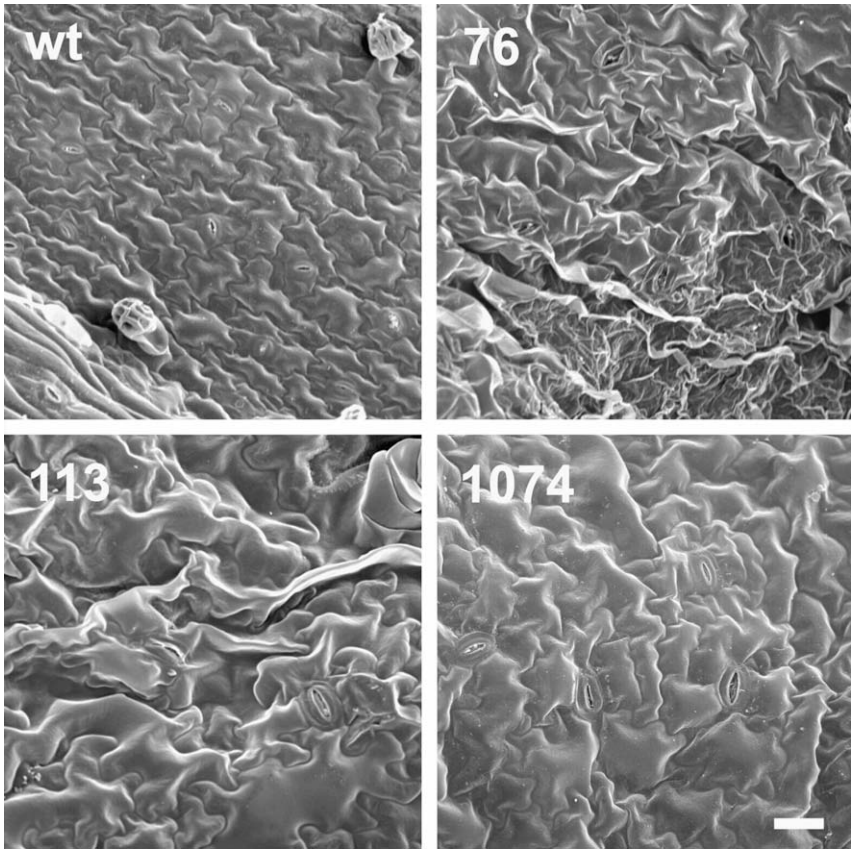

Fig. 7. Adaxial epidermal pavement cell appearance. Leaf samples at node 7 were prepared for SEM, fixed (Karnovsky's, see methods), dehydrated using ethanol, and critical point dried. Data are representative of 2–3 views each from a separate plant. All micrographs are of identical final magnification. Bar represent 50 μm.

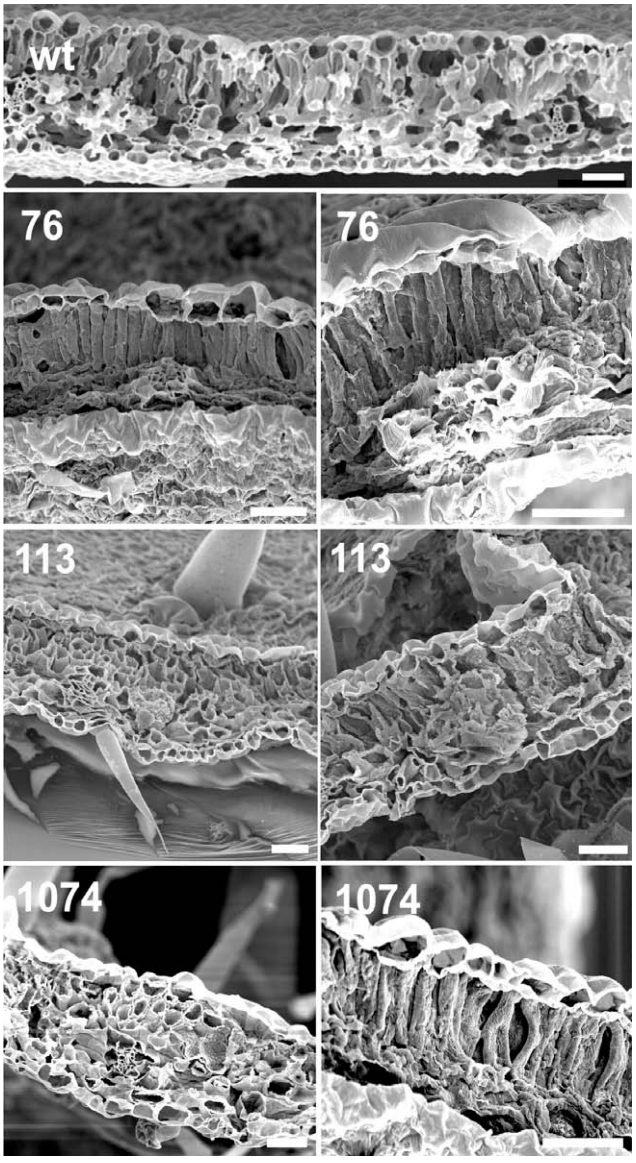

Fig. 8. Scanning electron microscopy of wt and transformed leaves. Images are representative of two to three samples taken from the leaf at node 7, from each of two to three plants per transgenic line. Bars represent 50 μm.

Table 5
Pigment content and photosynthetic rate of light green and dark green areas on leaves from transformed line 113.

	Leaf position and tissue color sampled		
	4 Dark/light	7 Dark/light	9 Dark/light
chl a (μg cm^{-2})	56.54/35.95	48.66/16.32	27.95/25.14
chl b (μg cm^{-2})	27.13/19.70	24.10/10.36	10.09/8.78
c (μg cm^{-2})	15.63/9.27	12.74/4.91	7.43/6.63
chl a/b (μg cm^{-2})	2.08/1.82	2.01/1.57	2.77/2.86
chl/c (μg cm^{-2})	5.35/6.0	5.71/5.43	5.11/5.11
PSR (μmol CO_2 min^{-1} cm^{-2})	ND	11.56/10.85	9.98/9.99

ND, not determined.
Note: chlorophyll a (chl a), chlorophyll b (chl b), and carotenoid (c) values represent pigment determinations carried out on a single leaf disc 5.78 mm in diameter punched from either a light green (light) area or an adjacent dark green (dark) area from a single leaf. Photosynthetic rate measurements (PSR) were carried out using a Li-Cor 6400 with a leaf enclosure chamber, the diameter of the enclosure greatly exceeded the diameters of the smaller light-green areas. Values displayed represent two to three measurements from dark green leaves and two measurements from light green patches in two mutant 113 plants.

effect of treatment on stomatal densities, with the mean stomatal densities on lines 113 and 1074 significantly lower at $p = 0.004$ and $p < 0.001$, respectively (Table 7).

3. Discussion

Significant progress has been made over recent years in engineering lignin. Initially much of this work aimed at improving pulp and paper-making through studies in model species such as tobacco and *Arabidopsis* and in wood and biomass species such as poplar (Anterola and Lewis, 2002; Boudet et al., 2003; Boerjan et al., 2003; Vanholme et al., 2008). This interest has now been extended to engineering renewable resources of biomass for optimized biofuel production from cell wall polysaccharides as an alternative to starch and sucrose and initial studies have demonstrated utility in Medicago (Chen and Dixon, 2007; Jackson et al., 2008). As part of these endeavours, a large amount of data has been accumulated that has positioned sufficient basic knowledge to allow further optimization of specific strategies in order to fully exploit such technology. From these initial studies, it is now realised that tissue specificity and regulation of the enzymes was operating in such a way that necessitated modification of earlier hypotheses and our understanding of these particular aspects of systems biology. This is best exemplified in the case of lignin where the pathway or metabolic grid has undergone considerable modification recently (Anterola and Lewis, 2002; Humphreys and Chapple, 2002; Boudet et al., 2003; Boerjan et al., 2003) and a number of questions have arisen from the initial studies of lignin manipulation that could

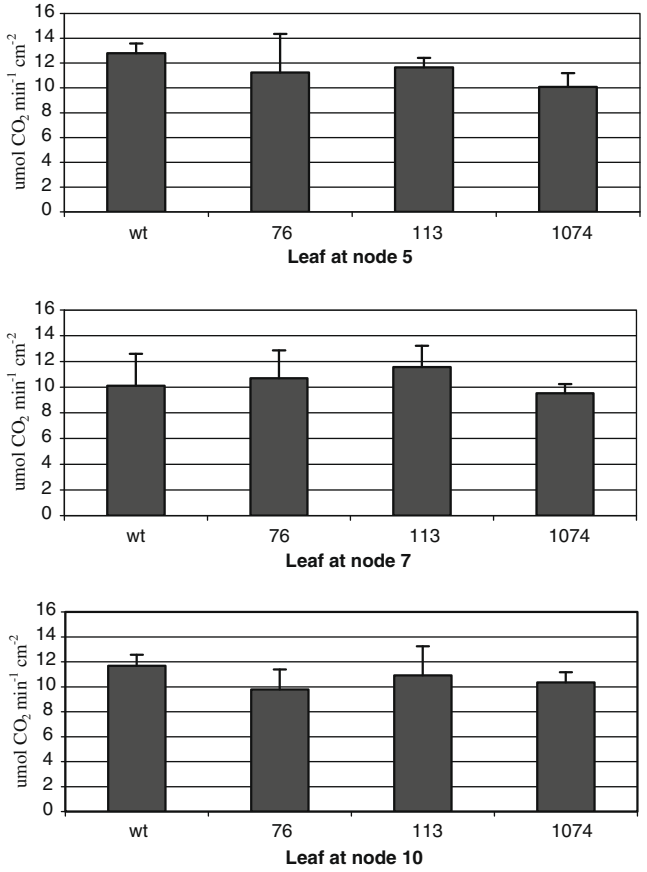

Fig. 9. Carbon dioxide fixation rates within developing tobacco leaves from wild type and transgenic plants. Replicate measurements of single leaf CO_2 fixation rates, from two of each of the representative plants were averaged. The experiments were carried out on leaves at nodes 5, 7, and 10. Error bars represent +1SD.

Table 6
Statistical analysis of carbon fixation rates shown in Fig. 9.

	Sum of squares	df	Mean-square	*F*-ratio	*p*
One-way ANOVA					
Between groups					
All lines at leaf 5	28.577	3	9.526	5.422	0.007
All lines at leaf 7	19.711	3	6.570	2.635	0.079
All lines at leaf 10	11.860	3	3.953	1.670	0.205
Plant	1074	113	76		wt
Bonferroni matix of pairwise comparison probabilities for carbon fixation rates at leaf 5					
1074	1.000				
113	0.303	1.000			
76	1.000	0.596	1.000		
wt	0.012	0.930	0.032		1.000

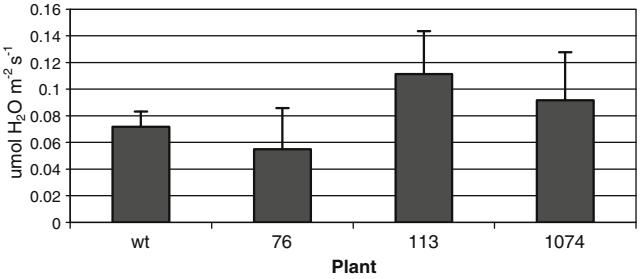

Fig. 10. Stomatal conductance of leaf 10 in wild type and transformed plants. Data represent averages of six measurements. Three measurements from different areas on each of two separate leaves, each leaf from one of two replicate plants. Measurements were made using Li-Cor 6400, on leaves at nodes 5, 7, and 10. However, the data presented represents average conductance in leaves at node 10 only. Error bars represent +1SD.

Table 7
Statistical analysis of stomatal conductance data from leaves at node 10 shown in Fig. 10.

	Sum of squares	df	Mean-square	*F*-ratio	*p*
One-way ANOVA					
Between groups					
All lines at leaf 10	0.011	3	0.004	4.174	0.019
Plant	1074	113	76		wt
Bonferroni matrix of pairwise comparison probabilities for conductance at leaf 10					
1074	1.000				
113	1.000	1.000			
76	0.251	0.020	1.000		
wt	1.000	0.179	1.000		1.000

affect performance of the resultant transgenic resource and these need to be addressed further. These include the influence of functional redundancy of biosynthetic enzymes and their complex regulatory mechanisms, the occurrence of compensatory mechanisms by other participants and the possible consequential un-intended or undesirable consequences of transgenesis. The present study further examines antisense lignification-specific peroxidase lines (Blee et al., 2003) for such changes in leaf and vascular tissue as part of this ongoing evaluation of optimum strategies for engineering new resources of biomass.

Most manipulation of lignin has been at the various levels of flux control into phenylpropanoids and formation of monolignols and therefore the type of lignin structure rather than polymerisation. From an analysis of the accumulated data for transformations (Anterola and Lewis, 2002), it would appear that manipulation of targets in the phenylpropanoid pathway, the earliest stage of lignin biosynthesis (PAL, C4H, 4CL, and C3H) in tobacco and *Arabidopsis*, reduces the lignin content and, with the exception of PAL, generally shows higher *G* to *S* ratios (Kajita et al., 1996; Sewalt et al., 1997; Blee et al., 2001a; Abdulrazzak et al., 2006). This may indicate that reduction of flux through the pathway leads to selective depletion of the intermediates that go through to *S* units and *G* units, since there is growing evidence that these pathways may be differentially regulated in different cell types. However, in the present study there was an increase in *S* over *G* units as shown by immunocytochemistry in the peroxidase down-regulated lines and, therefore, as a consequence of manipulation of the polymerisation step. This may indicate differential specificity of more than one peroxidase operating in vascular tissue and that TP60 may have more activity towards guaiacyl units. One possible other contributor to lignification is the tobacco anionic peroxidase, which was localised to the xylem parenchyma (Klotz et al., 1998), shows high activity in lignifying stem tissue (Lagrimini and Rothstein, 1987) and also catalyses wound induced lignification (Lagrimini, 1991). As an increase in *S* over *G* units has been found for tobacco lines down-regulated for PAL, it also indicates unpredictable variation between species and down-regulation of individual steps leads to different effects on the monomer composition of lignin. Similarly, down-regulation of the later enzymes of monolignol biosynthesis, coniferylaldehyde 5-hydroxylase (F5H), CCR and CAD (Chabannes et al., 2001a,b; O'Connell et al., 2002) leads to limited effects on total lignin but with drastic and opposing changes in *S*/*G* ratios (Anterola and Lewis, 2002).

Morphological analysis has shown a wide range of phenotypes in terms of the effect of transgenesis on the vasculature and on the type and distribution of lignin in these plants. In tobacco, C4H lines showed reduced xylem development and this was reflected in the walls where the S2 of vessels showed major changes. However, these lines did not seem particularly stable as homozygous lines we subsequently generated failed to show the same reduction of lignin reported for T_0 lines (Blee et al., 2001a). Changes in S2 were much more exacerbated for CCR lines and lignin was particularly poor in "condensed" guaiacyl and syringyl epitopes. Changes in S2 were not observed in CAD but immunolabeling showed the deposition of lignin was developmentally delayed (Chabannes et al., 2001a,b). In poplar (Ruel et al., unpublished data), lines down-regulated in COMT showed delayed lignification and wall irregularities in the S2 of vessels. As expected there was a decrease in syringyl residues. For CCOMT, there were no such profound changes, only an increase of guaiacyl epitopes in vessels and fibers. As for tobacco, the CCR lines showed major changes in S2 with the characteristic loosening phenotype (Chabannes et al., 2001a,b; Ruel et al., 2001). In this case, there was a conspicuous lack of 'non-condensed' syringyl residues in this layer.

We now present a similar analysis on peroxidase antisense lines. At the morphological level, the present results show that down-regulation of peroxidase affected xylem development by limiting secondary wall assembly in vessels. This suggests that if monolignols polymerisation is impaired, the growth of the secondary wall becomes limited. It is interesting that the specific impact on vessels points out a cell specificity of the peroxidase encoded by gene TP60. The developmental reduction of the S2 layer in the secondary thickening of the vessel walls does not support the suggestion that repression of lignin synthesis would be compensated by an enhanced synthesis of cellulose (Hu et al., 1999; Li et al., 2003), since this should have compensated for the loss of thickening material. In this respect, the absence of variation of the glucose to xylose ratio in xylem at any developmental stage in the tobacco lines contrasts with enhanced synthesis of cellulose (Hu et al., 1999; Li et al., 2003; Leplé et al., 2007) or reduction in hemicellulose (Leplé et al., 2007) reported for lignin down-regulation in tree species through targeting provision of monolignols. However, one must bear in mind that

the impact of peroxidase is tissue specific and that the carbohydrate analysis concerned the whole xylem tissue, therefore averaging the possible variations in the sole vessels (Angeles et al., 2006). Nevertheless, the combined wall changes demonstrated industrial utility in a more effective enzymatic saccharification of stem biomass of about threefold compared with wild-type.

These subtle changes in composition were surprising against the background of gene expression. The general down-regulation of the lignin pathway with the exception of CCR was in accordance with the reduction of lignin. Such changes in expression has been observed for other lignin down-regulated tobacco lines (Dauwe et al., 2007), although little is known about the feedback reduction that might control this. However, the increases in specific cellulose synthase and xylan pathway gene expression are not reflected in measurable increases in these polymers suggesting extra levels of control besides transcriptional activation. qRT-PCR used for these expression studies will not, of course, show silencing of the TP60 transcript since the methods and primers used will not differentiate between amplification of sense and antisense transcripts. In northern blots, an FBP1 probe (corresponding to constructs in lines 76 and 113) more strongly targeted a transcript most abundant in leaves, while the TP60 probe (lines 1074, 1120, and 1135) reacted more strongly to a transcript most abundant in stems (Blee et al., 2003). It is possible that antisense gene silencing using either FBP1 or TP60 could be targeting two peroxidase transcripts in tobacco. Similar antisense gene silencing methods in *Arabidopsis* using the FBP1 cDNA resulted in a measurable decrease in two transcripts (Bindschedler et al., 2006). However, when analysed at the protein level, a vascular-specific cationic peroxidase proved to be the protein target for silencing (Blee et al., 2003).

With respect to leaf morphology and anatomy, transformed lines 76, 113, and 1074 all displayed similar phenotypic abnormalities, possibly due to indirect effects of peroxidase gene silencing on developmental processes. Leaf primorida in tobacco consist of about four cell layers derived from the L1, L2, and L3 layers of the shoot apical meristem (Poethig and Sussex, 1985; Poethig, 1987). Cell divisions forming the leaf cease first in the epidermis, then in the lower mesophyll layers, and eventually in the upper mesophyll layer, which will generate palisade cells (Avery, 1933). Cells of the epidermis continue to expand after the middle and lower mesophyll stop (Avery, 1933). Forces generated by the epidermal expansion pull apart mesophyll cells to create the spongy mesophyll. Palisade cells of the upper mesophyll may also be pulled apart by the epidermal expansion. Palisade cells acquire a portion of their depth almost as soon as the leaf blade is initiated and are readily apparent as columnar cells by the time the leaf is 4–5 mm in length (Avery, 1933). We observed mesophyll regions within the leaves of lines 113 and 1074, which completely lacked the characteristic columnar expansion of the upper layers into palisade cells. Plant cell growth and expansion are supported by several enzymatic systems that loosen cross-links of the wall, including class III peroxidases (Passardi et al., 2005). More specifically in tobacco leaves, auxin-induced growth did not stimulate simultaneous acidification of the mesophyll cell wall or a change in membrane potential (Keller and Van Volkenburgh, 1998). Presumably cell wall loosening in tobacco leaves is not dependent on activation of acid-dependent cell wall loosening enzymes. Evidence is accumulating that indicate auxin-induced cell growth in some tissues is brought about through the generation of hydroxyl radicals (Schopfer et al., 2002). The plant class III peroxidases are hypothesized to function in both cell wall loosening and cross-linking through reactive oxygen species (ROS) generation and regulation, H_2O_2 level regulation, and oxidation of various substrates. ROS generated by peroxidases are capable of cleaving pectin and xyloglucan (Fry, 1998; Schweikert et al., 2000) and endogenous H_2O_2 levels have been correlated with the expansion processes and implicated peroxidases in cell growth (Passardi et al., 2004, 2005). In transformed lines 113 and 1074, loss of a peroxidase may have prevented ROS such as H_2O_2 levels required for cell loosening and expansion and/or schizogenic processes that would allow differential expansion of cell layers within the lamina to form well developed spongy and palisade mesophyll.

Transformed lines 76, 113, and 1074 also displayed occasional light green patches randomly within the leaf blade. Exposure of transgenic tobacco deficient in catalase to high light conditions resulted chlorosis and necrosis of the leaves (Chamnongpol et al., 1998). The lesions were attributed to a 90% reduction in activity for the H_2O_2 detoxifying enzyme catalase. Local events yielding excessive H_2O_2 levels in leaves of peroxidase mutant lines 76, 113, and 1074 may result in areas with reduced chlorophyll. These disturbances of developmental processes within the leaf resulted in a 21% reduction in carbon assimilation rates per unit surface area in line 1074 (wt at 12.8 μmol CO_2 min^{-1} cm^{-2} and line 1074 at 10.1 μmol CO_2 min^{-1} cm^{-2}).

Extensive profiling of respective CCR and CAD antisense down-regulated tobacco lines (Dauwe et al., 2007) established that, in addition, to down-regulation of the whole pathway leading to reduced lignin, photo-oxidative stress, elevated leaf chlorophylls a, b, and carotenoids, up-regulation of starch metabolism, and no apparent effect on CO_2 assimilation rate occurred. Although here we have also found down-regulation of phenylpropanoid pathway expression except for CCR, we found localised lowering of leaf chlorophyll a, b, and carotenoid levels, reduction of chloroplast diameter (see also Kavousi (2004)), and reduction of CO_2 assimilation rate. This might be consistent with additional functions of peroxidase already alluded to.

4. Concluding remarks

The present study increases knowledge of the utility of lignin modification for many processes. By increasing knowledge and gene discovery in the pathway, and therefore expanding the number of targets, it has proved possible to compare manipulation of lignin at the various levels of flux control, incorporation of monolignols and therefore the type of lignin structure, and regulation of polymerisation. In some cases, morphological changes can occur at the substructure level without any gross phenotypic changes. Therefore, a multidisciplinary analytical approach is therefore necessary to fully appreciate the subtlety of the consequences of transgenic manipulation of lignin even down to the molecular level.

5. Experimental

5.1. Plant materials

T_1 lines examined here were previously generated and expressed one of two antisense peroxidase constructs, each driven by the CaMV/35S promoter (Blee et al., 2003). Transgenic lines 76 and 113 represent the product of screening 81 plants expressing the antisense FBP1 (French bean) cDNA, while lines 1074, 1120, and 1135 were screened from 88 plants expressing the antisense TP60 (tobacco) cDNA. Briefly, T_0 lines were screened by southern blotting and transgene expression. T_1 lines were generated by selfing T_0 lines with single inserts and culture on selective medium. They were routinely clonally propagated before flowering stage. For in depth-studies studies of biotechnological applicability of modified stems, plants "homozygous" for one parent (tobacco being an allotetraploid), were successfully derived from two (1074 and 1120) of four main lines (1074, 1102, 1120, 1135) analysed in the previous studies.

5.2. Growth and sampling conditions

Lines were propagated vegetatively in the greenhouse at 16 h/8 h light–dark regime and average temperature of 25 °C. Stem material for analysis was taken just before flowering at around the 20-internode stage. Xylem tissue was isolated from designated internodes after separation of bark and pith by hand-dissection with a razor blade for each individual profiling parameter according to the protocol agreed by the partners in EU FPV COPOL (QLK5-2000-01493) and as outlined in related work previously (Chabannes et al., 2001a,b; O'Connell et al., 2002; Bindschedler et al., 2007; Dauwe et al., 2007; Millar et al., 2009).

5.3. Total hydrolysis of polysaccharides

Samples for carbohydrate analysis were the dried (lyophilised) lowest internodes from the stems. Three sections were cut corresponding to the top, the middle part, and the lower part of the internode. The xylem tissues were isolated by hand-dissection after removing the epidermis and the pith. Stem xylem composition was expressed as % of the whole internode based on dry weight (Table 2). Cell wall material was prepared by sequentially extracting the ground xylem tissues twice (10 min each) with each of the following, first with a mixture of toluene and ethanol (2:1, v/v), followed by hot H_2O and finally with EtOH. The resultant samples of cell wall material were freeze-dried. Hydrolysis was carried out in 72% (v/v) H_2SO_4 (6 h, 20 °C) followed by 1 M H_2SO_4 (4 h, 100 °C) in the presence of *myo*-inositol as internal standard (Chambat et al., 1997). After neutralisation with $BaCO_3$, the monosaccharides were converted to their alditol acetate derivatives and analysed by gas–liquid chromatography. Correction factors calculated from model compounds were applied.

5.4. Enzymatic saccharification assays

Stems consisting of the bottom six internodes were homogenized in pre-chilled acetone. The material recovered was air dried and ground in liq. N_2. The samples were subsequently washed with acetone, subjected to two successive extractions with $CHCl_3$:MeOH (2:1, v/v) and to a final acetone wash. The pellet was next treated with phenol/acetone/H_2O (2:1:1, v/v), washed three more times in acetone–H_2O (4:1) and dried under vacuum. Enzymatic treatment to remove starch with amylase and amyloglucosidase (5U in 1 M NaOAc) was followed by H_2O and acetone washes and dried under vacuum. This constitutes acetone-insoluble material (AIM).

Enzymatic saccharification of lignocellulosic material was according to the laboratory analytical procedure of the National Renewable Energy Laboratory (LAP-009). The methods were adapted from Chen and Dixon (2007) and Jackson et al. (2008). Extracts were pre-treated at 100 °C for 10 min and subsequently incubated at 50 °C in sodium citrate buffer (0.1 M, pH 4.8) with the antibiotics kanamycin (100 μg/ml), tetracycline (15 μg/ml) and gentamycin (25 μg/ml) and an enzyme cocktail consisting of driselase, cellulase from *Tricoderma reesei*, cellulase from *Aspergillus* spp. (all from Sigma–Aldrich, UK) and macerase (EMD Chemicals, Germany). The determination of total carbohydrates in untreated and pre-treated biomass was according to the Laboratory Analytical Procedure of the National Renewable Energy Laboratory (LAP-009). After a given length of time, the total sugars released into solution were estimated spectrophotometrically using the phenol–H_2SO_4 assay adapting the method from Dubois et al. (1956). The assay was optimized for 0.05 g of biomass in a total volume of 1 ml with 20 U of total cellulase. Under these conditions the time course was linear up to 72 h.

5.5. Immunocytochemistry

The specific polyclonal antibodies used were prepared and characterised as described by Joseleau and Ruel (1997). They were directed, respectively, against: syringyl (S) lignin polymer containing "non-condensed" inter-units linkages (Joseleau et al., 2004) and homoguaiacyl (Gzl) "condensed" lignin polymer. Immunolabeling in TEM was done on ultra-thin transverse sections (500 Å) taken from the lowest internode floating downward in plastic rings passed on 50 μl drops of reagents deposited on parafilm. The sections were first treated with 0.15 M glycine in Tris–HCl buffer 0.01 M, pH 7.6, containing 500 mM NaCl (TBS500), for blocking remaining aldehyde functions. This was followed by a 2 min rinse (×5) on TBS500. Protein–protein interactions were blocked for 30 min by incubating on 5% (w/v) non-fat dried milk in TBS500. The sections were then incubated on each antiserum diluted 1/50-1/100 in the blocking buffer. Incubation time was 3 h at room temperature followed by one night at 4 °C. After four washes (2 min each) in TBS500, followed by three rinses in Tris–HCl buffer (0.01 M Tris–HCl, pH 7.4–7.6), the sections were floated on the secondary marker [protein A-gold (pA 5), (Amersham)] diluted 1/25 in Tris–HCl buffer containing 0.2% fish gelatin for 90 min at room temperature. They were washed five times (2 min each) in Tris–HCl buffer and three times in H_2O. The sections were then post-fixed in 2.5% glutaraldehyde in H_2O and washed three times in H_2O. At this stage, the diameter of the 5 nm gold particles was further enhanced using a silver enhancing kit from Amersham. Finally, thin sections were transferred on carbon-coated copper grids and post-stained in 2.5% (v/v) aqueous uranyl acetate. Observations were performed at 80 kV with a Philips CM 200 Cryo-electron microscope. All comparative immunolabeling experiments were carried out in parallel in order to keep the same experimental conditions (dilutions of antibodies, times of contact, etc.) and pre-immune serum for each antibody was assayed on the different tobacco lines, in the same conditions as described for the immunogold labeling. The labeling in the transformed samples was expressed relative to that of the normal plant.

5.6. Leaf thickness, chlorophyll and carotenoid content measurement in developing leaves

Leaf thickness at nodes 4, 7, and 10 were measured using a digital caliper. In order to measure the chlorophyll and carotenoid content within a leaf, a hole-punch was used and two circular discs from each leaf were punched out and placed into an aluminum wrapped plastic scintillation vial containing 2 ml dimethylformamide. Samples were kept refrigerated over night and the next day samples were examined for pigment content. Samples were taken from leaves at node 3, 4, 7, and 10 (5.78 mm discs) and leaf at node 9 (7.5 mm discs) and absorbance of the pigment extracts was recorded at 480, 640, and 670 nm. Statistical comparison of average pigment content from five leaves was made using ANOVA and the Bonferroni pairwise test. The anatomy of the xylem of normal and transformed lines was examined with the ANOVA statistical analysis equipped with the program Kyplot (Kyenslab, Tokyo, Japan).

5.7. Carbon fixation measurement

The portable photosynthesis system, Li-Cor model 6400, (Li-Cor Corporate Office, 4421 Superior Street Lincoln, Nebraska) was used to measure rate of photosynthesis and stomatal conductance of green house grown plants for leaves at nodes 5, 7, and 10. Each leaf was measured in three different regions on the leaf in order to determine the rate of photosynthesis throughout the leaf. One measurement was taken from the right surface on the leaf blade,

the second one done on the opposite side and the third measurement conducted at the tip of the leaf. Photosynthesis was measured at a light level of 1600 μmol m^{-2} and at a controlled leaf temperature.

5.8. Tissue preparation for scanning electron microscopy

Leaves at node 5 were harvested from the plant, cut into pieces using a razor blade on a piece of dental wax, while immersed in fixative (2.5% paraformaldehyde, 2.5% glutaraldehyde, and 0.05% tween-20 in 50 mM sodium cacodylate pH7.4). Tissues were then washed with buffer (Sorenson's) then dehydration preceded using 50%, 70%, 90%, and two 100% (v/v) EtOH water mixtures at 37 °C for 40 s in a microwave. Then tissues were immersed into three 100% (v/v) series of dihexamethyldisilazane and placed inside a microwave (Pelco model 3440, Ted Pella, Inc., Redding, CA) at 37 °C for 40 s each time. Samples were dried at 60 °C in an oven for 15 min, and then allowed to cool down.

A second set of tissues were prepared using EtOH, and then critical point dried as follows; tissues were fixed, rinsed with Sorenson's buffer, and dehydrated using an EtOH concentration series of 50%, 70%, 95%, and 100% (v/v) twice. Then tissues were critical point dried. Tissues were coated with gold, and were then stored in a box for future examination with scanning electron microscopy images obtained from SEM were analysed using Carnoy software (Lab of Plant Systematics, K.U. Leuven, Flanders, Belgium), Adobe Photoshop 6.0 (Adobe Systems, Inc.), and Image Tool (Department of Dental Diagnostic Science, University of Texas Health Science Center, San Antonio).

5.9. RNA extraction

RNA was extracted from pooled xylem tissue taken from nodes 1 to 6 of 10 plants (c.f. Dauwe et al., 2007) with guanidium thiocyanate–phenol by a modification of the Chomczynsky and Sacchi (1987) method. Briefly, the tissue was frozen immediately in liquid N_2 and ground using a mortar and a pestle at 4 °C. The powder was homogenized in extraction buffer for 5 min (10 ml for 1 g of frozen tissue). The extraction buffer consist in 1 volume of phenol, 0.1 volume of 3 M NaOAC (pH 4.0) and 1 volume of 4 M guanidium thiocyanate, 25 mM Na-citrate pH 7.0, 0.5% N Lauryl sarcosine, 0.7% β-mercaptoethanol. The insoluble material was removed from the homogenization buffer by centrifugation at 1000*g* for 15 min. Then, 2 volumes of $CHCl_3$ were added, with samples centrifuged at 3000*g* for 15 min. The supernatant was recovered and RNA was precipitated by adding 1 volume of *i*-PrOH. After 10 min of incubation, the samples were centrifuged at 3000*g* for 30 min. The supernatant was discarded and the pellet washed with EtOH–H_2O (3:1), and then resuspended in 0.5% sodium dodecyl sulfate.

5.10. Real-time RT-PCR mRNA quantification

DNAse-digested total RNA was reverse transcribed to generate cDNA using the QuantiTect® Reverse Transcription kit (Qiagen, USA). The selected tobacco cDNAs (Table 1) were amplified using the Quantace Sensimix NoRef SYBR green master mix (Quantace, UK) to determine real-time mRNA quantification. Primers were designed spanning intron exon boundaries where possible from tobacco EST and cDNA sequences using the Primer3 oligonucleotide design web tool (Rozen and Skaletsky, 2000). Where these were inefficient, the EST was used to identify corresponding full-length clones in Genbank and these were used to design satisfactory primers. The primers used in this study are listed in Table 1. The relative expression levels of each gene were interpolated from standard curves generated from serial dilutions of cloned fragments of the genes of interest. Each gene was cloned using the pGEM-T Easy Vector System (Promega, USA). 18sRNA and EiF were used as house-keeping reference genes. The differences in expression profiles of the genes of interest were calculated by normalization to 18sRNA. Standard amplification protocols were used and carried out on the Corbett Research RG-6000 real-time PCR machine (Corbett Research, Australia). Reaction volumes of 20 μl were used for each run, which were performed in triplicate. Relative levels of transcripts were determined using established methods (Pfaffl, 2001).

Acknowledgments

GPB thanks the BBSRC (UK) for funding and GPB and J-PJ also thank the EC Framework V for funding through COPOL (QLK5-2000-01493). The EST sequencing and arraying mentioned was carried out by the Functional Genomics Facility headed by Professor Keith J. Edwards, Bristol University and is gratefully acknowledged. We thank Safina Khan for help with qRT-PCR.

References

Abdulrazzak, N., Pollet, B., Ehlting, J., Larsen, K., Asnaghi, C., Ronseau, S., Proux, C., Erhardt, M., Seltzer, V., Renou, J.-P., Ullmann, P., Pauly, M., Lapierre, C., Werck-Reichhart, D., 2006. A *coumaroyl-ester-3-hydroxylase* insertion mutant reveals the existence of non-redundant *meta*-hydroxylation pathways and essential roles for phenolic precursors in cell expansion and plant growth. Plant Physiol. 140, 30–48.

Angeles, G., Berrio-Sierra, J., Joseleau, J.-P., Lorimier, P., Ruel, K., 2006. Preparative laser microdissection and single-pot cell wall material preparation: a novel method for tissue-specific analysis. Planta 224, 228–232.

Anterola, A.M., Lewis, N.G., 2002. Trends in lignin modification: a comprehensive analysis of the effects of genetic manipulations/mutations on lignification and vascular integrity. Phytochemistry 61, 221–294.

Asada, K., 1999. The water–water cycle in chloroplasts: scavenging of active oxygens and dissipation of excess photons. Annu. Rev. Plant Biol. 50, 601–639.

Avery, G.S., 1933. Structure and development of the tobacco leaf. Am. J. Bot. 20, 565–592.

Bartel, B., 1997. Auxin biosynthesis. Annu. Rev. Plant Biol. 48, 51–66.

Bernards, M.A., 2002. Demystifying suberin. Can. J. Bot. 80, 227–240.

Bernards, M.A., Fleming, W.D., Llewellyn, D.B., Priefer, R., Yang, X., Sabatino, A., Plourde, G.L., 1999. Biochemical characterisation of the suberization-associated anionic peroxidase of potato. Plant Physiol. 121, 135–146.

Bernards, M.A., Summerhurst, D.K., Razem, F.A., 2003. Oxidases, peroxidases and hydrogen peroxide: the suberin connection. Phytochem. Rev. 3, 113–126.

Bindschedler, L.V., Wheatley, E., Gay, E., Cole, J., Cottage, A., Bolwell, G.P., 2005. Characterisation and expression of the pathway from UDP-glucose to UDP-xylose in differentiating tobacco tissue. Plant Mol. Biol. 57, 285–301.

Bindschedler, L.V., Dewdney, J., Blee, K.A., Stone, J.M., Asai, T., Plotnikov, J., Denoux, C., Hayes, T., Gerrish, C., Davies, D.R., Ausubel, F.M., Bolwell, G.P., 2006. Peroxidase dependent apoplastic oxidative burst in Arabidopsis required for pathogen resistance. Plant J. 47, 851–863.

Bindschedler, L.V., Tuerck, J., Maunders, M., Ruel, K., Petit-Conil, K., Danoun, S., Boudet, A.-M., Joseleau, J.-P., Bolwell, G.P., 2007. Modification of hemicellulose content by antisense down-regulation of UDP-glucuronate decarboxylase in tobacco and its consequences for cellulose extractability. Phytochemistry 68, 2635–2648.

Blee, K.A., Choi, J.W., O'Connell, A.P., Jupe, S.C., Schuch, W., Lewis, N.G., Bolwell, G.P., 2001a. Antisense and sense expression of cDNA coding for CYP73A15, a class II cinnamate 4-hydroxylase, leads to a delayed and reduced production of lignin in tobacco. Phytochemistry 57, 1159–1166.

Blee, K.A., Wheatley, E.R., Bonham, V.A., Mitchell, G.P., Robertson, D., Slabas, A.R., Burrell, M.M., Wojtaszek, P., Bolwell, G.P., 2001b. Proteomic analysis reveals a novel set of cell wall proteins in a transformed tobacco cell culture that synthesises secondary walls as determined by biochemical and morphological parameters. Planta 212, 404–415.

Blee, K.A., O'Connell, A., Schuch, W., Choi, J., Lewis, N.G., Bolwell, G.P., 2003. A lignin-specific peroxidase in tobacco whose antisense suppression leads to vascular tissue modification. Phytochemistry 64, 163–176.

Boerjan, W., Ralph, J., Baucher, M., 2003. Lignin biosynthesis. Annu. Rev. Plant Biol. 54, 519–546.

Boudet, A.-M., Kajita, S., Grima-Pettenati, J., Goffner, D., 2003. Lignins and lignocellulosics: a better control of synthesis for new and improved uses. Trends Plant Sci. 8, 576–581.

Chabannes, M., Ruel, K., Yoshinaga, A., Chabbert, B., Jauneau, A., Joseleau, J.-P., Boudet, A.-M., 2001a. In situ investigation of specifically engineered tobacco lignins reveals a differential impact of individual transformations on the patterns of lignin deposition, at the cellular and sub-cellular levels. Plant J. 28, 271–282.

Chabannes, M., Barakate, A., Lapierre, C., Marita, J., Ralph, J., Pean, M., Danoun, S., Halpin, C., Grima-Pettenati, J., Boudet, A.M., 2001b. Strong decrease in lignin content without significant alteration of plant development is induced by simultaneous down-regulation of cinnamoyl CoA reductase (CCR) and cinnamyl alcohol dehydrogenase (CAD) in tobacco plants. Plant J. 28, 257–270.

Chambat, G., Cartier, N., Lefèbvre, A., Marais, M.-F., Joseleau, J.-P., 1997. Changes in cell wall and extracellular polysaccharides during the culture cycle of *Rubus fruticosus* cells in suspension culture. Plant Physiol. Biochem. 35, 655–664.

Chamnongpol, S., Willekens, H., Moeder, W., Langebartels, C., Sandermann, H., VanMontagu, M., Inze, D., Van Camp, W., 1998. Defense activation and enhanced pathogen tolerance induced by H_2O_2 in transgenic tobacco. Proc. Natl. Acad. Sci. USA 95, 5818–5823.

Chen, F., Dixon, R.A., 2007. Lignin modification improves fermentable sugar yields for biofuel production. Nat. Biotechnol. 25, 759–761.

Chomczynsky, P., Sacchi, N., 1987. Single-step method of RNA isolation by guanidinium thiocyanate–phenol–chloroform extraction. Anal. Biochem. 162, 156–169.

Dauwe, R., Morreel, K., Goeminne, G., Gielen, B., Rohde, A., van Beeumen, J., Ralph, J., Boudet, A.-M., Kopka, J., Rochange, S.F., Halpin, C., Messens, E., Boerjan, W., 2007. Molecular phenotyping of lignin-modified tobacco reveals associated changes in cell-wall metabolism, primary metabolism, stress metabolism and photorespiration. Plant J. 52, 263–285.

Donaldson, L., 2001. Lignification and lignin topochemistry – an ultrastructural view. Phytochemistry 57, 859–873.

Dubois, M., Gilles, K.A., Hamilton, J.K., Rebers, P.A., Smith, F., 1956. Colorimetric method for determination of sugars and related substances. Anal. Chem. 28, 350–356.

Duroux, L., Welinder, K.G., 2003. The peroxidase gene family in plants; a phylogenetic overview. J. Mol. Evol. 57, 397–407.

Fry, S.C., 1998. Oxidative scission of plant cell wall polysaccharides by ascorbate-induced hydroxyl radicals. Biochem. J. 332, 507–515.

Gazaryan, I.G., Lagrimini, L.M., 1996. Tobacco anionic peroxidase overexpressed in transgenic plants: aerobic oxidation of indole-3-acetic acid. Phytochemistry 42, 1271–1278.

Gazaryan, I.G., Lagrimini, L.M., Mellon, F.A., Naldrett, M.J., Ashby, G.A., Thorneley, R.N., 1998. Identification of skatolyl hydroperoxide and its role in the peroxidase-catalysed oxidation of indol-3-yl acetic acid. Biochem. J. 333, 223–232.

Hu, W.-J., Hardling, S.A., Lung, J., Popko, J.L., Stokke, D.D., Tsai, C.J., Chiang, V.L., 1999. Repression of lignin biosynthesis promotes cellulose accumulation and growth in transgenic trees. Nat. Biotechnol. 17, 808–812.

Humphreys, J.M., Chapple, C., 2002. Rewriting the lignin roadmap. Curr. Opin. Plant Biol. 5, 224–229.

Jackson, L.A., Shadle, G.L., Zhou, R., Nakashima, J., Chen, F., Dixon, R.A., 2008. Improving saccharification efficiency of alfalfa stems through modification of the terminal stages of monolignol biosynthesis. Bioenergy Res. 1, 180–192.

Joseleau, J.-P., Ruel, K., 1997. Study of lignification by non invasive techniques in growing maize internodes – an investigation by Fourier transform infrared, cross-polarisation-magic angle spinning ^{13}C-nuclear magnetic resonance spectroscopy. Plant Physiol. 114, 1123–1133.

Joseleau, J.-P., Faix, O., Kuroda, K.-I., Ruel, K., 2004. A polyclonal antibody directed against syringyl epitopes of native lignins. C. R. Biol. 327, 809–815.

Kajita, S., Katayama, Y., Omori, S., 1996. Alterations in the biosynthesis of lignin in transgenic plants with chimeric genes for 4-coumarate: coenzyme A ligase. Plant Cell Physiol. 37, 957–965.

Kavousi, B., 2004. Physiological and Ultrastructural Analysis of Leaves in Response to Class III Peroxidise Antisense Gene Silencing. Merrill Library Holdings California State University at Chico. <http://opac.csuchico.edu/record=b1677282>.

Keller, C.P., Van Volkenburgh, E., 1998. Evidence that auxin-induced growth of tobacco leaf tissues does not involve cell wall acidification. Plant Physiol. 118, 557–564.

Keren, N., Berg, A., Van Kan, P.J.M., Levanon, H., Ohad, I., 1997. Mechanism of photosystem II photoinactivation and D1 protein degradation at low light: the role of back electron flow. Proc. Natl. Acad. Sci. USA 94, 1579–1584.

Klotz, K.L., Liu, T.-T.Y., Liu, L., Lagrimini, L.M., 1998. Expression of the tobacco anionic peroxidase gene is tissue-specific and developmentally regulated. Plant Mol. Biol. 36, 509–520.

Lagrimini, L.M., 1991. Wound-induced deposition of polyphenols in transgenic plants overexpressing peroxidase. Plant Physiol. 96, 577–583.

Lagrimini, L.M., Rothstein, S., 1987. Tissue specificity of tobacco peroxidase isozymes and their induction by wounding and tobacco mosaic virus infection. Plant Physiol. 84, 438–442.

Lagrimini, L.M., Joly, R.J., Dunlap, J.R., Liu, T.-T.Y., 1997a. The consequence of peroxidase overexpression in transgenic plants on root growth and development. Plant Mol. Biol. 33, 887–895.

Lagrimini, L.M., Gingas, V., Finger, F., Rothstein, S., Liu, T.-T.Y., 1997b. Characterization of antisense transformed plants deficient in the tobacco anionic peroxidase. Plant Physiol. 114, 1187–1196.

Leplé, J.C., Dauwe, R., Morreel, K., Storme, V., Lapierre, C., Pollet, B., Naumann, A., Kang, K.Y., Kim, H., Ruel, K., Lefèbvre, A., Joseleau, J.P., Grima-Pettenati, J., De Rycke, R., Andersson-Gunneràs, S., Erban, A., Fehrle, I., Petit-Conil, M., Kopka, J., Polle, A., Messens, E., Sundberg, B., Mansfield, S.D., Ralph, J., Pilate, G., Boerjan, W., 2007. Downregulation of cinnamoyl-coenzyme A reductase in poplar: multiple-level phenotyping reveals effects on cell wall polymer metabolism and structure. Plant Cell 19, 3669–3691.

Lewis, N.G., Yamamoto, E., 1990. Lignin: occurrence, biogenesis and biodegradation. Annu. Rev. Plant Physiol. 41, 455–496.

Li, L., Zhou, Y., Cheng, X., Sun, J., Marita, J.M., Ralph, J., Chiang, V.L., 2003. Combinatorial modification of multiple lignin traits in trees through multigene cotransformation. Proc. Natl. Acad. Sci. USA 100, 4939–4944.

Marjamaa, K., Kukkola, E.M., Fagerstedt, K.V., 2009. The role of xylem class III peroxidases in lignification. J. Exp. Bot. 60, 367–376.

Mehlhorn, H., Lelandais, M., Korth, H.G., Foyer, C.H., 1996. Ascorbate is the natural substrate for plant peroxidases. FEBS Lett. 378, 203–206.

Millar, D.J., Whitelegge, J.P., Bindschedler, L.V., Rayon, C., Boudet, A.-M., Rossignol, M., Borderies, G., Bolwell, G.P., 2009. The cell wall and secretory proteome of a tobacco cell line synthesising secondary wall. Proteomics 9, 2355–2372.

O'Connell, A., Holt, K., Piquemal, J., Grima-Pettenati, J., Boudet, A., Pollet, B., Lapierre, C., Petit-Conil, M., Schuch, W., Halpin, C., 2002. Improved paper pulp from plants with suppressed cinnamoyl-CoA reductase or cinnamyl alcohol dehydrogenase. Transgenic Res. 11, 495–503.

Passardi, F., Penel, C., Dunand, C., 2004. Performing the paradoxical: how plant peroxidases modify the cell wall. Trends Plant Sci. 9, 1360–1385.

Passardi, F., Cosio, C., Penel, C., Dunand, C., 2005. Peroxidases have more functions than a swiss army knife. Plant Cell Rep. 24, 255–265.

Passardi, F., Tognolli, M., De Meyer, M., Penel, C., Dunand, C., 2006. Two cell wall associated peroxidases from Arabidopsis influence root elongation. Planta 223, 965–974.

Pfaffl, M.W., 2001. A new mathematical model for relative quantification in real-time RT-PCR. Nucleic Acids Res. 29, 2002–2007.

Poethig, R.S., 1987. Clonal analysis of cell lineage patterns in plant development. Am. J. Bot. 74, 581–594.

Poethig, R.S., Sussex, I.M., 1985. The developmental morphology and growth dynamics of the tobacco leaf. Planta 165, 158–169.

Rozen, S., Skaletsky, H., 2000. Primer3 on the WWW for general users and for biologist programmers. In: Krawetz, S., Misener, S. (Eds.), Bioinformatics Methods and Protocols: Methods in Molecular Biology. Humana Press, Totowa, NJ, pp. 365–386.

Ruel, K., Chabannes, M., Boudet, A.-M., Legrand, M., Joseleau, J.-P., 2001. Reassessment of quantitative changes in lignification of transgenic tobacco plants and their impact on cell wall assembly. Phytochemistry 57, 875–882.

Schopfer, P., Liszkay, A., Bechtold, M., Frahry, G., Wagner, A., 2002. Evidence that hydroxyl radicals mediate auxin-induced extension growth. Planta 214, 821–828.

Schweikert, C., Liszkay, A., Schopfer, P., 2000. Scission of polysaccharides by peroxidise-generated hydroxyl radicals. Phytochemistry 53, 565–570.

Sewalt, V.J.H., Ni, W., Blount, J.W., Jung, H.G., Masoud, S.A., Howles, P.A., Lamb, C.J., Dixon, R.A., 1997. Reduced lignin content and altered lignin composition in transgenic tobacco down-regulated in expression of L-phenylalanine ammonia-lyase or cinnamate 4-hydroxylase. Plant Physiol. 115, 41–50.

Tognolli, M., Penel, C., Greppin, H., Simon, P., 2002. Analysis and expression of the class III peroxidase large gene family in *Arabidopsis thaliana*. Gene 288, 129–138.

Valerio, L., De Meyer, M., Penel, C., Dunand, C., 2004. Expression analysis of the Arabidopsis peroxidase multigene family. Phytochemistry 65, 1331–1342.

Vanholme, R., Morreel, K., Ralph, J., Boerjan, W., 2008. Lignin engineering. Curr. Opin. Plant Biol. 11, 278–285.

Welinder, K.G., 1992. Superfamily of plant, fungal and bacterial peroxidases. Curr. Opin. Struct. Biol. 2, 388–393.